AD-A131 891 PERFORMANCE ANALYSIS OF A THREE-DIMENSIONAL MICROWAVE LENS IN A CYLINDRIC..(U) NAVAL RESEARCH LAB WASHINGTON DC H P COLEMAN ET AL. 29 JUL 83 NRL-8713 1/2

UNCLASSIFIED SBI-AD-E000 538 F/G 9/1 NL

END
DATE FILMED
9 83
DTIC

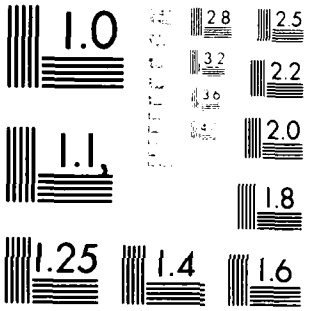

(2)

NRL Report 8713

Performance Analysis of a Three-Dimensional Microwave Lens in a Cylindrical Array Scanning Application

H. PARIS COLEMAN AND J. PAUL SHELTON

Electromagnetics Branch
Radar Division

July 29, 1983

NAVAL RESEARCH LABORATORY
Washington, D.C.

SECURITY CLASSIFICATION OF THIS PAGE (When Data Entered)

REPORT DOCUMENTATION PAGE	READ INSTRUCTIONS BEFORE COMPLETING FORM
1 REPORT NUMBER NRL Report 8713 2 GOVT ACCESSION NO	3 RECIPIENT'S CATALOG NUMBER
4 TITLE (and Subtitle) PERFORMANCE ANALYSIS OF A THREE-DIMENSIONAL MICROWAVE LENS IN A CYLINDRICAL ARRAY SCANNING APPLICATION	5 TYPE OF REPORT & PERIOD COVERED Interim report on a continuing NRL problem 6 PERFORMING ORG REPORT NUMBER
7 AUTHOR(s) H. Paris Coleman and J. Paul Shelton	8 CONTRACT OR GRANT NUMBER(s)
9 PERFORMING ORGANIZATION NAME AND ADDRESS Naval Research Laboratory Washington, DC 20375	10 PROGRAM ELEMENT, PROJECT, TASK AREA & WORK UNIT NUMBERS 53-0624-0 61153N; RR0210543
11 CONTROLLING OFFICE NAME AND ADDRESS Office of Naval Research NRL NSF Program Washington, DC 22217	12 REPORT DATE July 29, 1983 13 NUMBER OF PAGES 16
14 MONITORING AGENCY NAME & ADDRESS(if different from Controlling Office)	15 SECURITY CLASS. (of this report) UNCLASSIFIED 15a DECLASSIFICATION DOWNGRADING SCHEDULE

16 DISTRIBUTION STATEMENT (of this Report)

Approved for public release; distribution unlimited.

17 DISTRIBUTION STATEMENT (of the abstract entered in Block 20, if different from Report)

18 SUPPLEMENTARY NOTES

19 KEY WORDS (Continue on reverse side if necessary and identify by block number)

Navigation
Antenna
Circular array
Electronic scan

20 ABSTRACT (Continue on reverse side if necessary and identify by block number)

The calculated performance of a scanning cylindrical antenna array using a three-dimensional lens systems as the feed system is discussed. Nominal specifications of 4° beamwidth, 0.1° pointing accuracy and 25-dB sidelobe level were established. The system was designed to scan through a full 360° of azimuth using associate phase shifters and sector-switching matrix.

It is shown that the evaluated lens system is unable to meet the sidelobe specification and suffers in this regard, and with regard to overall system loss, when compared to a more conventional matrix feed system.

DD FORM 1 JAN 73 1473 EDITION OF 1 NOV 65 IS OBSOLETE
S/N 0102-014-6601

SECURITY CLASSIFICATION OF THIS PAGE (When Data Entered)

CONTENTS

PERFORMANCE ANALYSIS OF A THREE—DIMENSIONAL MICROWAVE LENS IN A CYLINDRICAL ARRAY SCANNING APPLICATION

INTRODUCTION

This report describes the calculated performance of a three-dimensional mircrowave lens used as a feed system for a scanning cylindrical array. The system is designed to scan a beam, in fine angular increments, through 360° in azimuth. Normally, a feed system for such an array might consist of multibeam matrix networks or two-dimensional lenses, possibly in combination with switching networks [1].

It has been shown that, under idealized circumstances, a multibeam three-dimensional lens is equivalent to multibeam matrices and two-dimensional lenses [2]. The use of a three-dimensional lens in scanning a cylindrical array is a particularly attractive possibility since, unlike an air dielectric, two-dimensional lens, it is sufficiently small to fit within the cylindrical array and, compared to a matrix, is relatively simple in construction.

For purposes of evaluation, the lens and cylindrical array are studied in the context of a proposed FAA microwave landing system (MLS) application. The performance of the lens system is compared with the performance of a perfect matrix system. The FAA application requires that a beam with a shaped elevation pattern be scanned to any azimuth position with an accuracy of 0.1°. A normal azimuth half-power beamwidth of 4° and a nominal sidelobe level of 25 dB are additional requirements. Design considerations for the 360° azimuth MLS antenna were discussed in a previous report [3].

Although the objective of this report is to evaluate the performance of a particular lens in a particular scanning cylindrical array configuration and *not* to describe the rationale for selecting this configuration, a brief qualitative discussion of the design problem is given here. The primary design problem in scanning a cylindrical array, once we have determined the aperture distribution to give the desired radiation pattern characteristics, is the rotation of the aperture distribution around the periphery of the array. In contrast to scanning a linear or planar array, in which the element phases are changed while the amplitudes are held constant, both amplitude and phase are changed, for each element of the cylindrical array. Furthermore, it can be shown that superior pattern performance is obtained only by simultaneous, continuous variation of both amplitude and phase. Varying phases while holding amplitudes constant to move the beam through a small angle, then jumping amplitudes abruptly is *not* a high-performance approach—thus, the complexity of the feed network. References 1, 3, 7, and 8 provide more detail for the interested reader. Designs showing the desired capability to rotate (or commutate) the distribution around the array are illustrated in this report.

A cylindrical array consisting of 37 vertical staves and fed by a 37-port, three-dimensional lens through an array of switches is the configuration selected for study. It is demonstrated that the desired beamwidth and pointing accuracy are attainable with this system. Inherent phase and amplitude errors in the lens preclude, however, the attainment of the desired sidelope levels. Furthermore, space attenuation and spillover losses in the lens produce a significant system loss.

Manuscript approved February 28, 1983.

LENS CONFIGURATION

The evaluated lens design consists of two arrays, each consisting of 37 elements, positioned so that their phase centers lie on equal-radius spherical surfaces. The center of each spherical surface is located on the other one. This arrangement is diagrammed in Fig. 1. Figure 2 shows the arrangement of the elements in each array. The arrangement is such that the phase centers form a regular hexagonal lattice when projected on a plane normal to the centerline of the lens. The interelement spacing, S, is constant in this projection. The top and bottom arrays are displaced relative to one another about the centerline of the lens by an angle γ. The design of lenses of this configuration is discussed in [2]. In the present instance, the design frequency is 5060 MHz and R, S and γ equal 56.46 cm (22.23 in.), 7.95 cm (3.13 in.) and 4.72° respectively.

The radiating elements in the arrays must be circularly polarized and some attention was given to selecting the design of a suitable antenna element so that performance of the lens system would be adequately modeled. The element selected was a helicone antenna [4] consisting of a 6.5-turn helix situated in a cone of 7.62-cm (3 in.) aperture, having a height of 10.16 cm (4 in.) and a base diameter of 5.08 cm (2 in.). This element exhibits good circularity—both on and off axis—and has clean radiation patterns which minimize spillover and cross-coupling to neighboring elements in the arrays. The one-tenth power beamwidth of this element is 90°. The pattern shape was approximated in the calcualtions by:

$$\text{LOG } P(\theta) = \left(\frac{\theta}{\theta_{10}}\right)^2$$

$P(\theta)$ is the power at an angle θ off the axis of the element and θ_{10} is the value of θ where the power is 0.1 of the on axis value. The power gain of the element was determined to be closely given by:

$$G_P = \frac{30\,000}{(\theta_3)^2},$$

where θ_3 is the half-power beamwidth in degrees. For the helicone described, this gives a gain of 10.9 dB. Since the interelement spacing is only 7.87 cm (3.1 in.), a substantial increase in gain of the lens element over this value is not possible.

A correspondence between ports on the lens surfaces and the ports of a Butler matrix [5,6] may be established [2]. Feeding the elements one by one on, say, the bottom surface of the lens gives a set of excitations on the elements of the opposite surface that approximate the excitation modes [7] obtained from a Butler matrix that has a zero-order mode. Ideal excitations would be uniform in amplitude and vary linearly in phase over the elements. In the case of 37 elements, perfect modes would be given by:

$$E_n = e^{j(2mn\pi/37)},$$

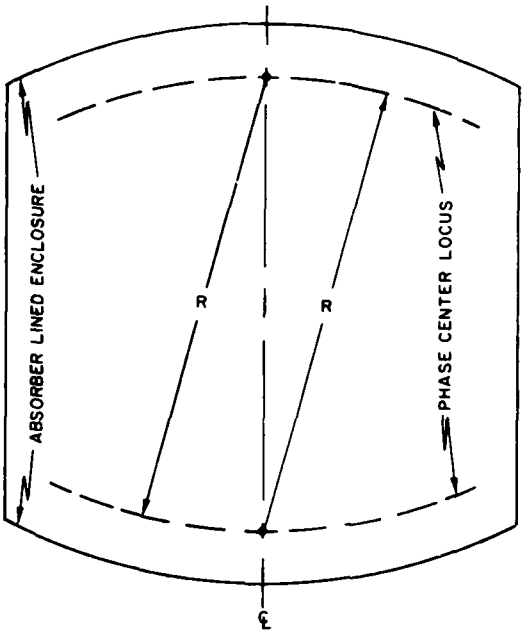

Fig. 1 — Lens geometry

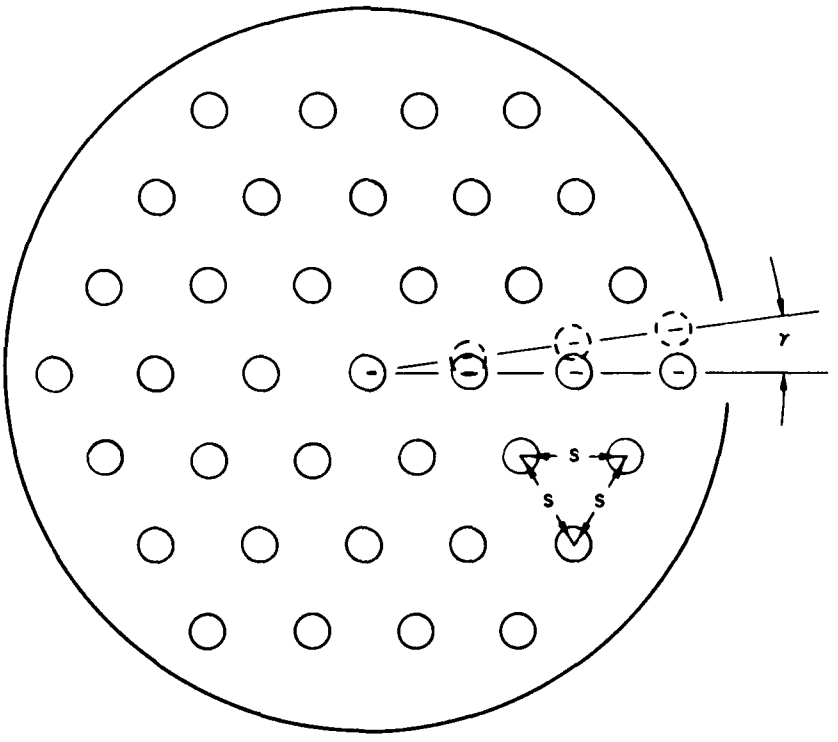

Fig. 2 — Arrangement of lens radiating elements

where n is the element number ($-18 \leq n \leq 18$) and m is the mode number ($-18 \leq m \leq 18$). In actuality, departures from these ideal excitations are unavoidable in the case of a lens. Amplitude errors occur as a result of differences in separation distance between elements of the two arrays and the effect of the radiation patterns of the elements in the arrays. Phase errors result from inherent collimation errors in the lens. These amplitude and phase errors only vanish for the central feed port (i.e., the zero mode). Plots of the calculated phase and amplitude errors of the lens described, as compared to a perfect matrix, are shown in Fig. 3. The phase error is independent of the beamwidth of the lens elements. The amplitude errors are, however, related to this beamwidth. The plot shown assumes a 90° tenth-power beamwidth for the lens element (as described above). For wider beamwidths, the peak amplitude, taken over all the modes, is dominated by the terms due to differences in spacing between elements of the top and bottom lens arrays and remains essentially at the peak value shown in the figure. Since lens attenuation is increased if wider beamwidth elements are used, there would be no performance benefit in using wider beamwidth elements.

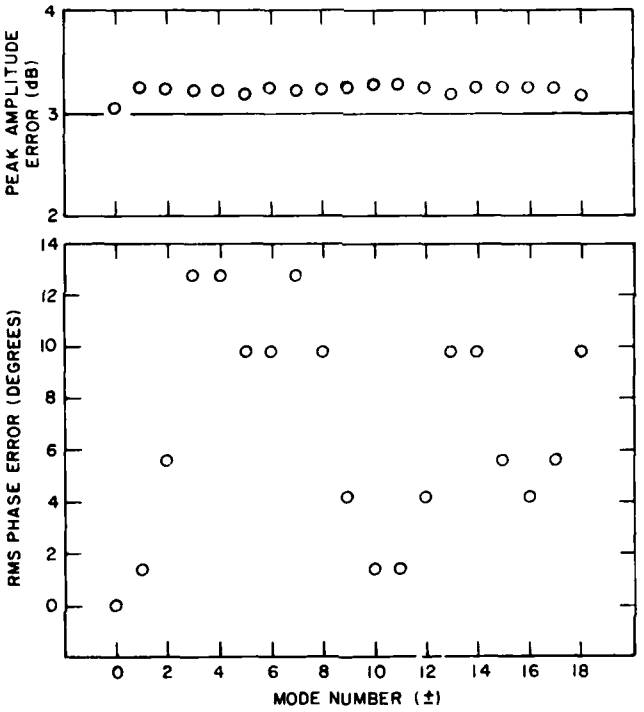

Fig. 3 — Lens phase and amplitude errors

SCANNING OF THE CYLINDRICAL ARRAY

The investigated scanning system is derived from the use of a Butler matrix as a commutation switch [1]. A diagram of such a commutation system is shown in Fig. 4. Assuming the set of variable phase shifters to be set to zero phase shift, a desired distribution may be established on the elements of the circular array by means of the power divider and set of fixed phase shifts. This distribution may then be moved around the array by linear variation of the variable phase shifters. The distribution returns to the initial position on the array when the variable phase shifts return to zero modulo 2π. This commutation property of the Butler matrix has been shown to be unique [8].

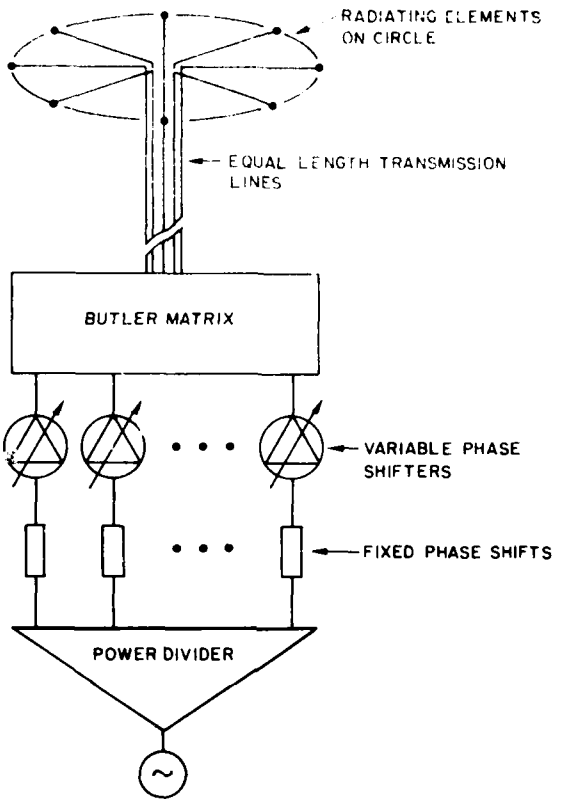

Fig. 4 — A Butler matrix as a commutation switch

As described above, full 360° scanning of a circular array having N elements is provided with an N-port matrix and N adjustable phase shifters. The scanning system can be extended to larger circular arrays without increasing the number of ports in the matrix, or the number of phase shifters, by using Q sectors each containing N elements and adding N switches to select which N of the elements are energized at a particular time. The switches are then N-pole, Q-throw, devices. A diagram of such a system for $N = 3$ and $Q = 3$ is shown in Fig. 5. The elements of the array, which would actually be arranged on the perimeter of a circle, are diagrammed as linearly arranged for convenience of explanation. Originally all switches are in their number one position. The phase shifters may be adjusted linearly so that the original element distribution is moved to the right in the figure. At the point where the distribution is moved over by one-half an element spacing, the first switch is thrown to its second position. This disconnects the first element in the first sector and adds the first element in the second sector. The linear variation in phase shifts may then be continued until the distribution is recentered on the new array of connected elements. Continuing adjustment of the phase shifters past this point, we next must throw the second switch to drop the leftmost element and add a new element on the right. Thus, when we use the linear variation of the input phase and successively change the switches to drop an element on the left and add an element on the right, the original distribution is moved around the perimeter of the larger array.

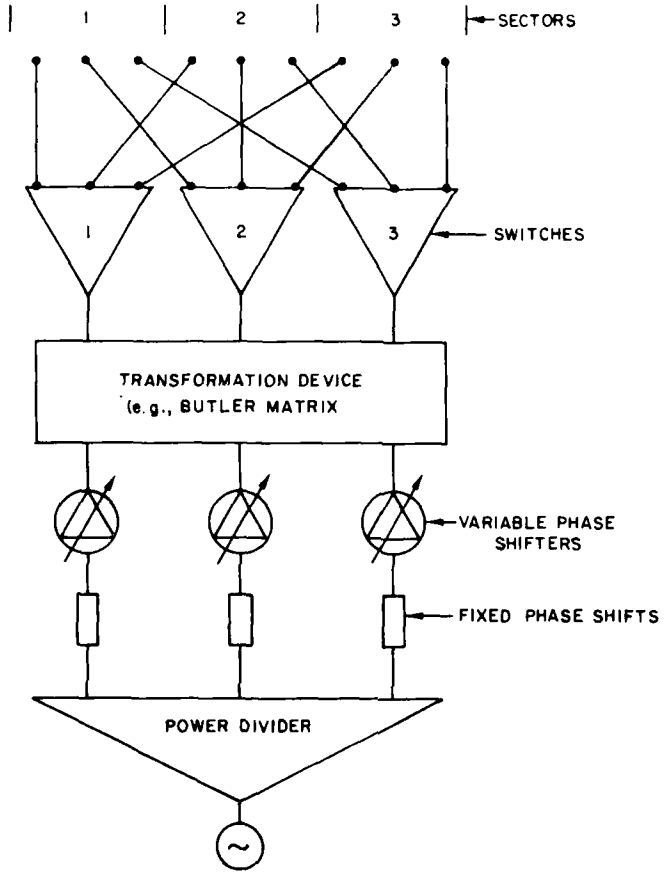

Fig. 5 — Commutation switch for a multisectored array

When the distribution is shifted so that it appears in its original form on a group of N elements we say the array is steered to a cardinal, or principal, beam position. Intermediate positions are considered as steered plus or minus a fine steering angle from these positions. Fine steering is accomplished by adjustment of the phase shifters only, but selection of a new principal beam position requires a new switch pattern in addition to adjustment of the phase shifters. Use of a Butler matrix with continuously variable phase shifters would theoretically result in the same radiation patterns at every principal beam position (except for the desired change in direction). Only these positions satisfy the commutation property. Intermediate (fine steered) positions do not, of course, replicate the original distribution on any group of elements and departures from the principal beam performance occurs. The performance with fine steering would, however, be identical about any principal beam position.

The array geometry investigated consists of 111 elements arranged in three sectors of 37 elements each. The first stage in evaluating the performance of this array configuration is the determination of suitable initial feeding coefficients for the 37 elements of the array that compose a single sector. This determination is discussed in the next section.

DETERMINATION OF ELEMENT COEFFICIENTS

Initial (unscanned) element distributions were derived from linear Taylor distributions [9]. These Taylor distributions are specifically designed to yield low sidelobes from linear apertures and may only be approximated in the case of an array located on a circular sector. Approximations were obtained by using a cophasal projection of a Taylor distribution on a linear aperture tangent to the circular array. This arrangement is shown in Fig. 6. Only the distribution from the center over one-half of the array need be considered. The distribution over the remaining elements may then be obtained by imaging around the central element. The distribution $G(X_n)$ at the point (X_n, ρ) was obtained by linear interpolation between values at 20 equally spaced points between $X = O$ and $X = X_{max}$. These values were obtained from tabulated values for the Taylor distributions [9]. Amplitude corrections were applied for element positions as α_n increases. The amplitude corrections were such that, if a uniform distribution were initially assumed on the tangential aperture, uniform power density would be obtained by backward projection from the elements of the array. Element pattern shape (see Fig. 6) was assumed to be of the form

$$F(\alpha_n) = (1 + \cos\alpha_n)^p.$$

A value of $p = 2$ gives good agreement with measured element patterns of edge slot arrays in the presence of neighboring terminated elements. Applying the several corrections discussed we obtain for the element coefficients:

$$E(\alpha_n) = \frac{\exp\,[j\beta\rho(1 - \cos\alpha_n)]}{\cos^2(\alpha_n) \cdot (1+\cos\alpha_n)^p} \cdot G(\rho\sin\alpha_n),$$

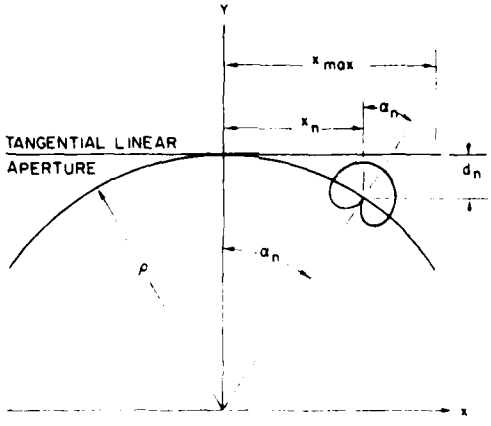

Fig. 6 — Geometry of array sector as used to obtain element excitations

where ρ is the radius of the array, α_n is the angle to the n^{th} element, and $\beta = 2\pi/\lambda_O$. The value of λ_O is the wavelength at the design frequency.

An objective of 30 dB was set for calculated sidelobes from the array with the initial (unscanned) distribution. This allows for some deterioration with scan before a nominal 25-dB sidelobe level is exceeded. Figure 7 shows a calculated pattern for the unscanned circular section array. This pattern was obtained by using an order-6 Taylor distribution with 35-dB sidelobes (for a linear aperture) as the objective function $G(X_n)$. The radius of the array was adjusted so that the sidelobes in the rearward direction (shown as dotted in the figure) did not exceed the maximum sidelobe in the forward direction (shown solid). The design frequency was fixed at 5060 MHz, and the value of ρ = 59.81 cm (23.55 in.) is attainable with edge slot radiators in waveguide. This initial distribution was used in the majority of subsequent calculations evaluating the scanning performance of the array.

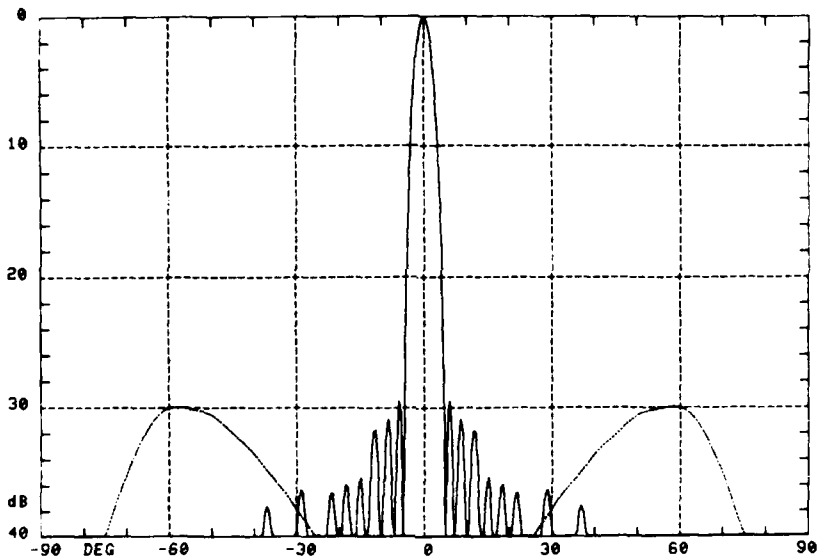

Fig. 7 — Unscanned radiation pattern of sector of cylindrical array with element excitations derived from a 35-dB linear Taylor distribution

DETERMINATION OF FEED COEFFICIENTS

After we determine the distribution over the elements of the sectorial array, the feeding coefficients at the input terminals of the transformation device (lens or matrix) may be determined. For an odd number of elements, $N = 2L + 1$:

$$E_n = \sum_{m=-L}^{L} C_m T_{m,n} \text{ for } -L \leqslant n \leqslant L,$$

where E_n is the n^{th} element coefficient, C_m is the m^{th} input coefficient, and $T_{m,n}$ is the complex transfer coefficient between the m^{th} and n^{th} port. By use of the symmetries of the problem:

$$E_n = C_O T_{O,n} + \sum_{m=1}^{L} C_m (T_{-m,n} + T_{m,n}), \; 0 \leq n \leq L.$$

This is a set of $L + 1$ simultaneous equations in the $L + 1$ unknowns, C_m. With the transfer coefficients and the element coefficients known, this set may be solved for the set of C_m.

EVALUATION OF SCANNED BEAM CHARACTERISTICS

In evaluation of the lens performance, the scanning system of the cylindrical array discussed earlier and diagrammed in Fig. 5 was numerically simulated for the cylindrical array consisting of three sectors, each with 37 radiating elements. Radiation patterns were calculated in 0.5° increments of far field angle for a number of beam positions. The main beam maximum, left and right half-power points, and the level of the highest sidelobe were obtained by quadratic interpolation between the calculated pattern points. Beam position was determined by averaging the left and right half-power points. Directivity was calculated by using Simpson's rule. In all calculations, perfect construction of the system was assumed; thus, only the effects of inherent errors are included. The performance of the system incorporating the lens is compared with the performance when a lossless 37-element Butler matrix is substituted for the lens.

Figure 7 shows the unscanned pattern of the array with the 35-dB linear Taylor distribution as the objective function. This pattern is the same for either a lens or matrix feed system. The set of mode excitation coefficients (i.e., the power diversion of the power divider and the values of fixed phase shifts diagrammed in Fig. 5) differs, of course, for the two cases. Both systems are, however, scanned by the same settings of variable phase shifters and switches. The two systems show significant differences in scanned pattern performance. Figures 8 and 9 show the radiation patterns of the matrix system and the lens system scanned half way to the next principal beam position. Figure 10 graphs the maximum sidelobe level for both systems fine steered about the zero principal beam position. Differences between the two systems are small. The performance of the matrix system, however, is cyclic with a period equal to the spacing between principal beams and, therefore, the sidelobes with this system never are worse than shown here. The performance of the lens system, however, is cyclic with a period of 120° (for a three-sector array) and significant deterioration in performance occurs as the beam is steered through the various principal beam positions. Sidelobe level as the beam is fine steered around the 18th principal beam position is also shown in Fig. 10.

Figure 11 shows the sidelobe level for the lens and matrix systems for a sample set of random beam positions. These positions were established by choosing a random fine steering fraction around each of the principal beam positions that are associated with one third of the array, and are therefore representative of all beam positions encountered in steering the array through a full 360°. The rapid deterioration of sidelobe level of the lens-fed system with scanning is apparent from this figure.

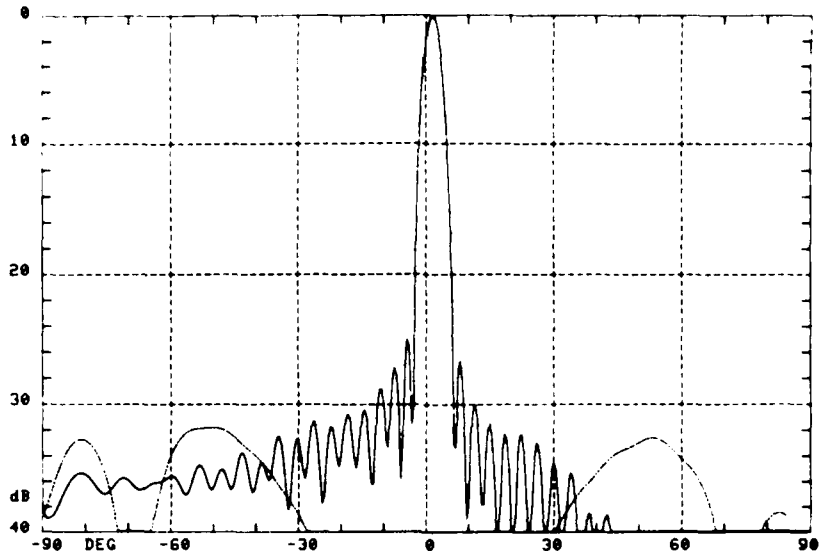

Fig. 8 — Pattern of matrix-fed system fine-steered by 0.5 from the 0-beam position

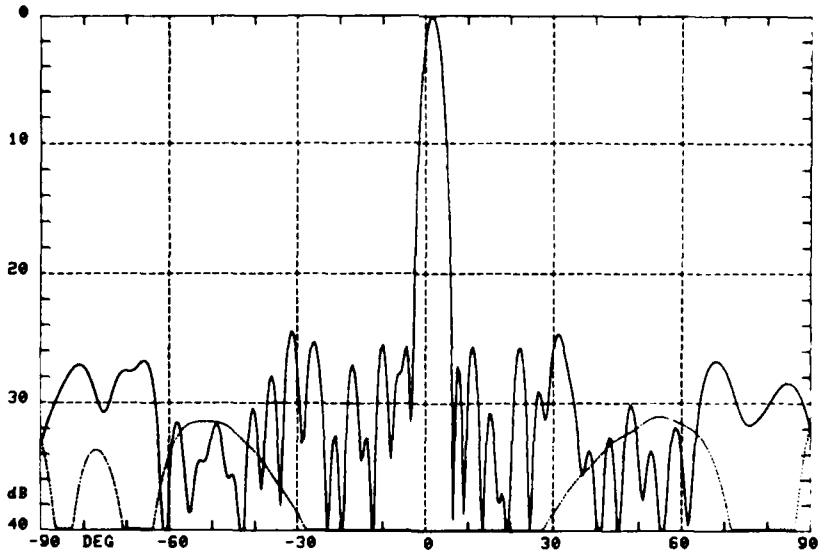

Fig. 9 — Pattern of lens-fed system fine-steered by 0.5 from the 0-beam position

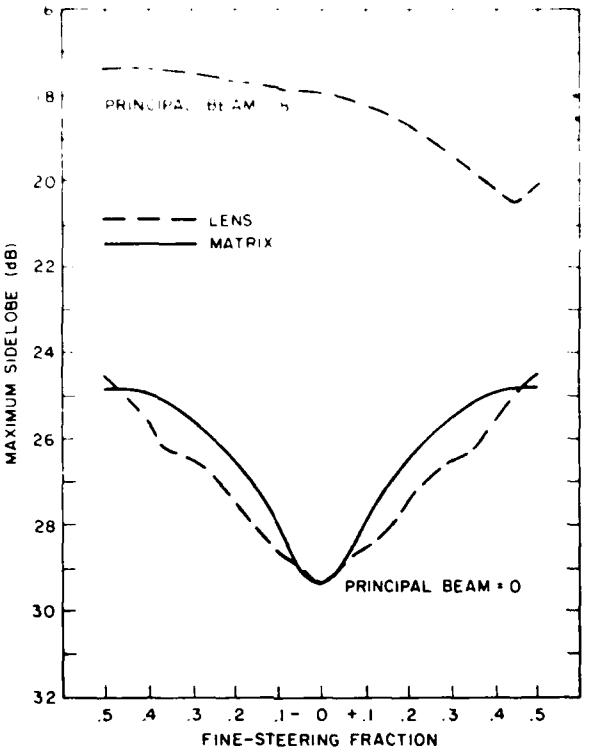

Fig. 10 — Sidelobe level *vs* fine steering

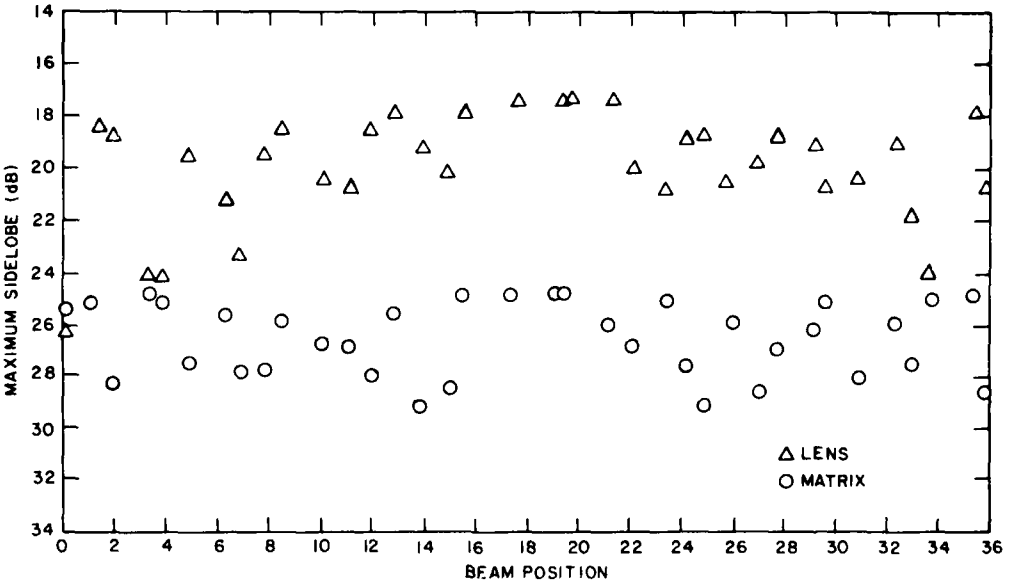

Fig. 11 — Sidelobe levels for random beam positions (lens and matrix systems)

Tables 1a and 1b statistically summarize the various data obtained from the calculated patterns for the matrix system and the lens system using a 90° tenth-power beamwidth lens element. Beam pointing error and beamwidth for both systems are acceptable. The sidelobe level for the lens system, however, is much too high. Table 1c summarizes the pattern data when an isotropic radiator is assumed for the lens feed. There is no significant improvement in sidelobe level in this case, and the lens' mean loss is increased from 7.33 dB to 25.83 dB with this change.

Table 1 — Order 6 Linear Taylor distribution—35-dB Sidelobe

(a) Scan evaluation using perfect matrix	Maximum	Mean	Sigma
Sidelobe (dB)	24.78	26.41	1.47
Pointing error (deg)	0.05	0	0.04
Beamwidth (deg)	—	3.75	0.04
Directivity (dB)	—	19.58	0.05
System loss (dB)	—	0	0
(b) Scan evaluation using lens Lens element 10th power beamwidth of 90°	Maximum	Mean	Sigma
Sidelobe (dB)	17.36	19.92	2.17
Pointing error (deg)	0.07	0	0.03
Beamwidth (deg)	—	3.61	0.07
Directivity (dB)	—	19.47	0.08
System loss (dB)	—	7.33	0.29
(c) Scan evaluation using lens Lens element an isotropic radiator	Maximum	Mean	Sigma
Sidelobe (dB)	18.25	20.72	1.98
Pointing error (deg)	0.09	0.01	0.04
Beamwidth (deg)	—	3.70	0.04
Directivity (dB)	—	19.46	0.06
System Loss (dB)	—	25.83	0.12

Figure 12 shows plots of cumulative normal distributions for the lens and matrix systems. These plots are based upon the sample means and standard deviations given in Table 1. There is, of course, no reason to assume normal distribution of maximum sidelobe and this figure is presented merely as an aid in comparing the performance of the scanning systems. Superimposed plots of the actual sample cumulative probability distributions, however, indicate that a comparison made in this way is reasonably accurate. The performance deficiency of the lens system is apparent from this figure, which shows that a maximum sidelobe less than 25 dB would only be obtained for less than one percent of the beam positons of the lens system. An additional distribution is shown on this figure for the case of an order 6 linear Taylor objective function with 40-dB sidelobes. The unscanned pattern for this case is shown in Fig. 13. The choice of the lower sidelobe objective function is seen to have little effect on the overall sidelobe performance of the lens scanning system.

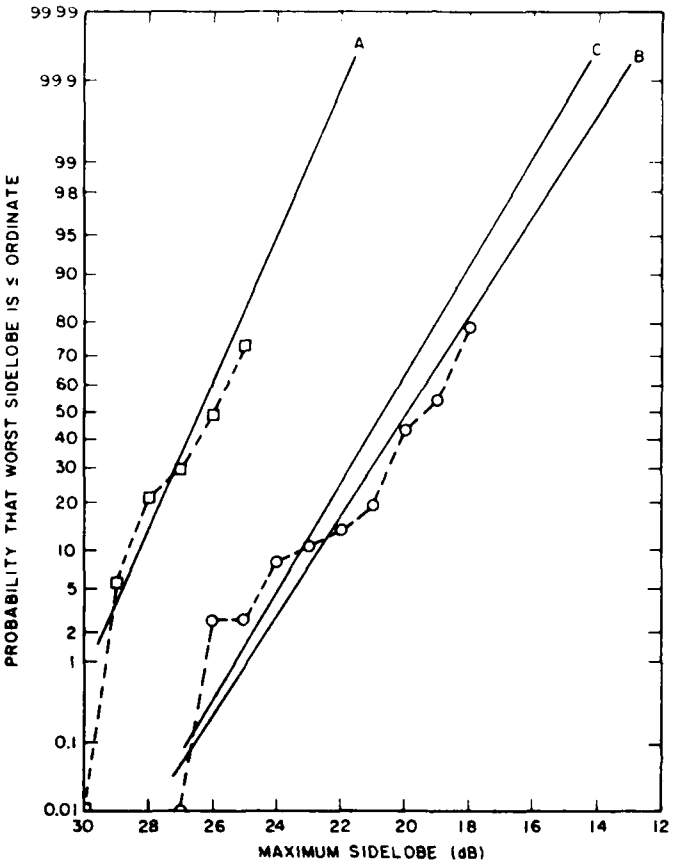

Fig. 12 — Cumulative normal probability distribution plots of maximum sidelobe levels. Curve A — linear 35-dB Taylor objective, matrix fed, □ - - - □ corresponding actual sample distribution, curve B — linear 35-dB Taylor objective, lens fed ○ - - - ○ corresponding actual sample distribution, and curve C — linear 40-dB Taylor objective, lens fed.

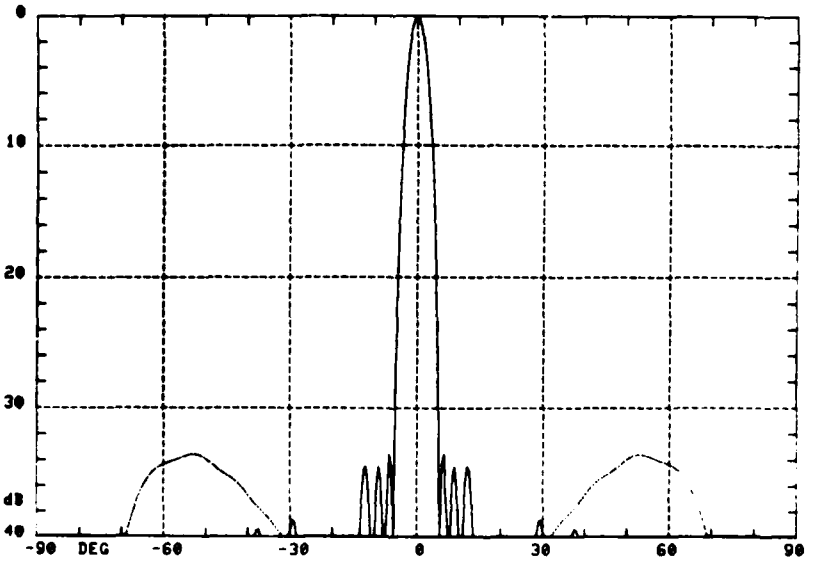

Fig. 13 — Unscanned radiation pattern of sector of cylindrical array with element excitations derived from a 40-dB linear Taylor distribution

CONCLUSIONS

It has been demonstrated that sidelobe levels attainable from the three-dimensional lens-fed cylindrical array cannot meet the desired 25-dB level. Pointing accuracy of 0.1° is, however, attainable with the system as designed. The lens' mean loss of 7.33 dB may be compared with an estimated loss of 3 dB for a roughly equivalent matrix. The equivalent matrix is taken as a network with 36 inputs and outputs and six layers of directional couplers, with 0.5-dB insertion loss for each directional coupler.

ACKNOWLEDGMENT

The contributions of Mr. Billy D. Wright of the Electromagnetics Branch, in experimentally verifying the parameters associated with the lens feed and array element, are gratefully acknowledged.

REFERENCES

1. A. E. Holley, E. C. Dufort and R. A. Dell-Imagine, "An Electronically Scanned Beacon Antenna," Transactions of the IEEE, Antennas and Propagation, AP-22, No. 1, 3-12, Jan 1974.

2. J. P. Shelton, "On the Equivalence of Two-Dimensional and Three-Dimensional Multibeam Microwave Lenses," NRL Report 8493, 17 Jul 1981.

3. J. P. Shelton and J. K. Hsiao, "Summary Report on NRL Participation in the Microwave Landing System Program," NRL Memo Report 4305, Appendix H, Aug. 1980.

4. K. R. Carver, "The Helicone — A Circularly Polarized Antenna with Low Sidelobe Level," Proc. IEEE, 55, No. 4, p 559, April 1967.

5. J. P. Shelton and K. S. Kelleher, "Multiple Beams from Linear Arrays," Transactions of the IRE, Antennas and Propagation, AP-9, No. 2, 154-161, Mar 1961.

6. J. Butler and R. Lowe, "Beam-Forming Matrix Simplifies Design of Electronically Scanned Antennas," Electronics Design 9, 170-173,12 Apr 1961.

7. B. Sheleg, "A Matrix-Fed Circular Array for Continuous Scanning," Proceedings of the IEEE, 56, No. 11, 2016-2027, Nov 1968.

8. R. M. Brown, "The Uniqueness of the Butler Matrix as a Commutating Switch," Transactions of the IEEE, Antennas and Propagation, AP-18, No. 5, 694-695, Sept 1971.

9. *Microwave Scanning Antennas*, I (APERTURES), Ed. R. C. Hansen, 94-97 and 419-421 Academic Press, 1964.

END

DATE
FILMED

9-83

DTIC